ACS APPLIED MATERIALS & INTERFACES

Research Article

www.acsami.org

Surface Characterization of the Carbon Cathode and the Lithium Anode of Li−O_2 Batteries Using $LiClO_4$ or LiBOB Salts

Reza Younesi,* Maria Hahlin, and Kristina Edström

Department of Chemistry - Ångström Laboratory, Uppsala University, Box 538, SE-751 21 Uppsala, Sweden

ABSTRACT: The surface compositions of a MnO_2 catalyst containing carbon cathode and a Li anode in a Li−O_2 battery were investigated using synchrotron-based photoelectron spectroscopy (PES). Electrolytes comprising $LiClO_4$ or LiBOB salts in PC or EC:DEC (1:1) solvents were used for this study. Decomposition products from $LiClO_4$ or LiBOB were observed on the cathode surface when using PC. However, no degradation of $LiClO_4$ was detected when using EC/DEC. We have demonstrated that both PC and EC/DEC solvents decompose during the cell cycling to form carbonate and ether containing compounds on the surface of the carbon cathode. However, EC/DEC decomposed to a lesser degree compared to PC. PES revealed that a surface layer with a thickness of at least 1−2 nm remained on the MnO_2 catalyst at the end of the charged state. It was shown that the detachment of Kynar binder influences the surface composition of both the carbon cathode and the Li anode of Li−O_2 cells. The PES results indicated that in the charged state the SEI on the Li anode is composed of PEO, carboxylates, carbonates, and $LiClO_4$ salt.

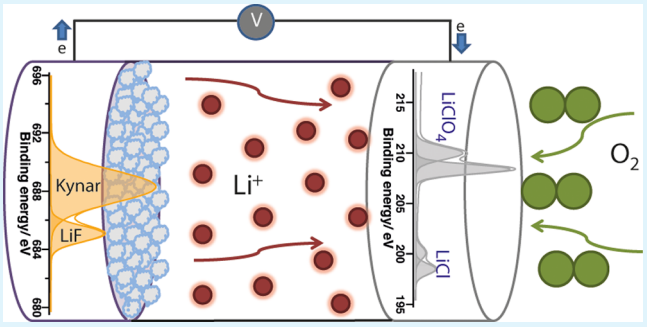

KEYWORDS: *lithium-air, Li anode, photoelectron spectroscopy, synchrotron, XPS, oxygen battery, lithium perchlorate, lithium bis(oxalato)borate*

1. INTRODUCTION

To overcome the concerns about today's energy production based on fossil fuel, researchers need to further develop sustainable renewable energy sources such as wind, solar, and hydro power combined with effective chemical energy storage systems like batteries. The emergence of the novel and advanced lithium battery technology has raised hopes for this development as one way to tackle the problem of too large quantities of greenhouse gas emissions as well as to decrease the dependency on oil.

To fulfill the increased demands of efficient large storage, lithium batteries need to be improved considerably. Therefore, a vast amount of research is going on around the world to increase the specific energy (gravimetric energy density) and the energy density (volumetric energy density). In this respect, the Li−O_2 battery (often called the lithium-air battery) has lately attracted much attention due to its high specific energy (theoretically ten times that of a conventional Li-ion battery).

The Li−O_2 battery comprises a metallic lithium anode (or possibly a lithium alloy) and a porous carbon cathode containing a catalyst. In a nonaqueous Li−O_2 cell, lithium ions react with reduced oxygen species and form lithium peroxide and/or lithium oxide (Li_2O_2/Li_2O) as the final discharge product.[1] Currently, large research efforts are taken to overcome the crucial issues of the Li−O_2 battery, such as: the electrolyte stability, the synthesis of effective catalysts, the optimization of a porous cathode structure, etc.[2−5]

Several types of catalysts including metal oxides, precious, and nonprecious metals have been investigated with the aim to increase the discharge capacity or the rechargeability of the Li−O_2 battery.[4−6] However, it is still questionable if a catalyst will accelerate the formation and the oxidation of Li_2O_2 or if it rather will catalyze the decomposition of the electrolyte.[7,8] To study the catalytic activity of different catalysts, researchers should establish a truly reversible oxygen reduction and oxygen evolution reaction without any other side reactions. However, because of the instability of the solvents and lithium salts in different electrolyte tested so far, further research on catalysts are somewhat hampered.

From studies of Li-ion batteries, it has been shown that the anion of the lithium electrolyte salt influences the chemical composition and thermal stability of electrode/electrolyte interfaces.[9,10] We have recently shown that the $LiPF_6$ salt decomposes in Li−O_2 cells during cell cycling.[11] Similar results have also been reported by Veith et al.[12] They also investigated the stability of several different lithium salts including $LiBF_4$, LiTFSI, and $LiClO_4$ and suggested that $LiClO_4$ is the more stable. Beside these salts, $LiB(CN)_4$ and LiBOB salts have also been proved to decompose during the cycling of Li−O_2 cells.[13,14] All these mentioned salts are mostly stable in conventional Li-ion batteries. Thus, it can be anticipated that

Received: November 7, 2012
Accepted: January 21, 2013
Published: January 21, 2013

the decomposition of the lithium salts in the Li−O_2 battery originates from reactions with the oxygen ions and trace amounts of water. It has been shown that the super oxide radical (O_2^-), which is the intermediate oxygen reduction product in the Li−O_2 battery, is highly reactive.[15,16] The electrolyte decomposition in Li−O_2 cells has mainly been explained as originating from the attacks by this radical. Therefore, also lithium salts are most likely to be instable in contact with the O_2^-. In addition, Li_2O_2, which is a strong oxidizing agent, can decompose lithium salts.[17−20] Overall, finding a new lithium salt or stabilizing an existing lithium salt is still a dilemma for the Li−O_2 battery. Herein, we in detail study the stability of two nonfluorinated salts, $LiClO_4$ and LiBOB, in Li−O_2 cells because these salts have been tested to be some with the highest stability so far.

To resolve the issue of solvent instability, many different types of electrolytes including aprotic organic solvents, polymer electrolytes, ionic liquids, etc., have already been investigated for the Li−O_2 battery.[21−26] However, aprotic organic solvents and particularly alkyl carbonate-based ones, like propylene carbonate (PC), have been used more than other types of solvents because they are relatively simpler, cheaper, and safer. Nevertheless, most of these solvents decompose by reactions with O_2^- resulting in the formation of lithium carbonate (Li_2CO_3), lithium alkyl carbonates ($ROCO_2Li$), and Li acetate, etc., on the cathode side during the discharge of the battery.[11,16,26−30]

Although recent studies have shown that PC decomposes when cycling the Li−O_2 battery, there is still a need to investigate the stability of other types of carbonate-based electrolytes that have been shown to be more stable in Li-ion batteries. In this study we chose the solvent of ethylene carbonate/diethyl carbonate (EC/DEC) for the investigation of its performance and of surface layers formed on both cathode and lithium-anode during the battery cycling. Herein, the surfaces formed during cycling in EC/DEC cells are compared with those formed in a PC-based cell. We have observed that EC/DEC, compared to PC, shows a higher stability in contact with Li_2O_2.[17]

Despite the detrimental reactions between O_2^- and the electrolyte influencing the surface of the cathode, only few studies have been devoted to electrolyte decomposition on the Li anode side of the cell in the presence of oxygen.[31] We have earlier shown that compared to a nonoxygen cell, PC breaks down to a larger extent on the surface of a Li anode in the presence of oxygen resulting in the formation of an unstable solid electrolyte interphase (SEI) which is constantly evolving during cell cycling.[31] Therefore, we also include a study of the surface composition of Li anodes cycled using $LiClO_4$ in EC/DEC or PC electrolytes to understand the role of the salt for the decomposition processes.

Synchrotron-based Photoelectron Spectroscopy (PES), which is one of the most effective techniques for studying the outermost surfaces of compounds, was used in this study. PES can be used not only to detect crystalline but also amorphous chemical compounds on the surface of electrodes to depths of several nanometers. In this study, we selected to use relatively low excitation photon energies to study shallow depths of the surfaces of the electrodes. This can hence be seen as a complementary method to conventional Al Kα X-ray photoelectron spectroscopy (XPS) for the surface characterization of cathode and anodes in Li−O_2 cells.[11,31]

2. EXPERIMENTAL SECTION

Li−O_2 cells were assembled within an argon-filled glovebox (O_2, H_2O < 2 ppm) using a modified Swagelok design with an opening allowing oxygen to access through the cathode (Figure 1). Lithium foil was used as the negative electrode, Solupor as the separator, and a porous cathode as the positive electrode to assemble the cells. The porous cathodes were made of carbon Super P (Lithium battery grade, Erachem Comilog), Kynar 2801 (Arkema) as binder, and α-MnO_2 nanotubes as catalyst in weight ratios of 25:33:42 (cathode weight: ∼3 mg). α-MnO_2 nanotubes were synthesized according to reference.[32] To synthesize α-MnO_2 nanotubes, 10 mmol concentrated HCl (Merck) and 2.5 mmol $KMnO_4$ (J.T. Baker) dissolved in 70 mL of deionized water were hydrothermally heated at 140 °C for 12 h in a 100 mL of sealed Teflon-lined stainless steel autoclave (Parr Instrument Co.). After the autoclave was cooled down naturally to room temperature, the obtained precipitates were collected by centrifugation and then washed with deionized water and ethanol, separately. Prior to use, the cathodes were dried at 120 °C overnight in a vacuum furnace placed within the glovebox. One M $LiClO_4$ in EC:DEC (1:1) or in PC and 1 M LiBOB in PC were used as electrolytes. All the solvents were purchased from Ferro, Purolyte, with water contents ≤5 ppm as measured by Karl Fischer titration. The cells were kept in special designed airtight containers with inlet and outlet valves to purge ultra clean oxygen gas (Figure 1). The containers were initially filled with a continuous relatively high flow of dry oxygen for about 0.5 h. The open circuit voltage (OCV) of the cells was measured inside of the Argon-filled glovebox after the assembly but also outside of the glovebox after the initial filling of the cells with oxygen. After that, the cells were filled with a continuous relatively slow flow of dry oxygen for an extra 1 h rest time before the cycling. The OCV of the cells were again recorded before starting the discharge. A current density of 70 mA/g (based on the amount of carbon in the cathode) was applied using a Digatron BTS-600. To analyze the surface of the carbon cathode and the Li anode at the charged state, the cells were run and stopped when the cell voltage was ∼0.2 V higher than the voltage of charge plateau; the cells containing $LiClO_4$ in EC/DEC and PC electrolytes were stopped at 4.1 and 3.9 V, respectively, whereas the cell containing LiBOB in PC electrolyte was stopped at 4.3 V.

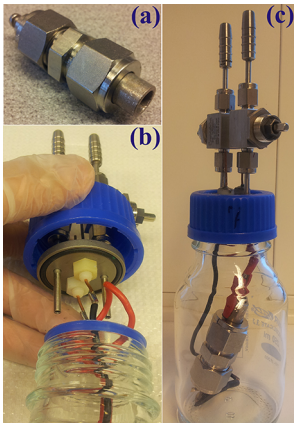

Figure 1. Modified Swagelok design with (a) an opening to atmosphere and (b, c) a special designed airtight container with inlet and outlet valves.

The cells were dismantled in the Argon-filled glovebox, after which, both the cathode and anode were washed with few drops of dimethyl carbonate to remove remaining species on the samples. This washing is vital for obtaining PES spectra from surface layers formed on the samples rather than from remaining electrolyte species. Washing the samples is also helpful for avoiding unwanted reactions between the electrolyte and the electrodes during sample transfer from glovebox to PES analyzing chamber. This is especially important when a sample is

transferred to synchrotron facilities, which substantially increases the transfer time. In this study, the samples were transported to the Swedish synchrotron MAX-IV Laboratory in Lund in vacuum-sealed polymer-coated aluminum bags to protect them against air and moisture contaminations. Each bag was opened in an argon-filled glovebox (H_2O < 1 pm) at the MAX IV Laboratory, and then the samples were mounted in a specially designed transfer chamber and transported to the analyzing chamber without exposure to the atmosphere. The measurements were performed using synchrotron radiation (beamline I-411) at the MAX IV Laboratory. Photons were monochromatized by a Zeiss SX-700 plan grating monochromator. A kinetic energy (E_K) of 140 eV was used for all the XPS measurements, implicating that the excitation photon energy ($h\nu$) was changed from 200 to 835 eV depending on the binding energy (E_B) of the measured core level, thus resulting in the same analysis depth for all the elements. The F 1s, O 1s, B 1s and Cl 2p spectra were energy calibrated using the hydrocarbon peak at 285.0 eV. The Mn 2p and Li 1s spectra were energy calibrated using survey scans. The spectra were intensity normalized to 1. Curve fitting was performed using IGOR Pro 4.0.7, and a linear background was subtracted before the spectra were deconvoluted. The morphologies of pristine and cycled cathode were obtained using a scanning electron microscopy (SEM) micrograph LEO 1550.

3. RESULTS AND DISCUSSION

First the electrochemical performance of the assembled Li−O_2 cells is presented. This is followed by a surface analysis of the carbon cathodes and Li anodes of the cells.

3.1. Cycling Profiles. Discharge/charge profiles of the first cycle of Li−O_2 cells assembled and cycled using 1 M $LiClO_4$ in EC/DEC, 1 M $LiClO_4$ in PC or 1 M LiBOB in PC electrolytes are presented in Figure 2. The profiles of the $LiClO_4$-based cells

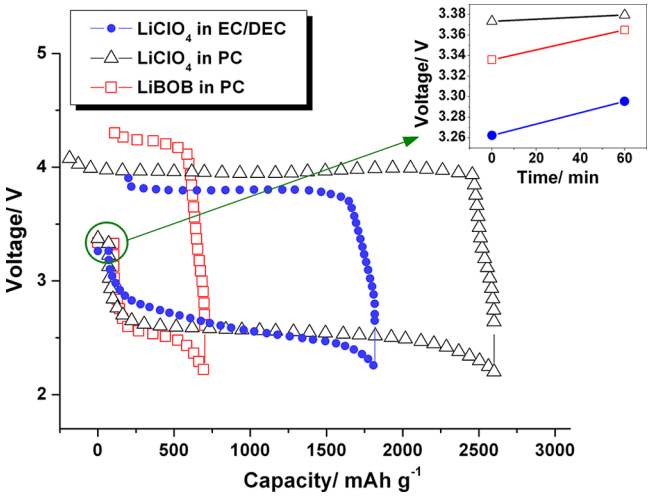

Figure 2. Discharge/charge profile of 1st cycle of Li−O_2 cells using 1 M $LiClO_4$ in EC/DEC, 1 M $LiClO_4$ in PC, or 1 M LiBOB in PC electrolytes. Inset: the increase in the OCV of the cells during the rest time before discharging.

show that $LiClO_4$ in PC performed with a higher discharge capacity (~2500 mA h g^{-1}; calculated based on the amount of carbon in the cathode) than the cell with $LiClO_4$ in EC/DEC (~1800 mA h g^{-1}). The charge capacity of the "$LiClO_4$ in PC" cell is higher than its discharge capacity suggesting electrolyte side reactions. Compared to the $LiClO_4$ based batteries, the cell with LiBOB in PC exhibited a smaller discharge capacity (~700 mA h g^{-1}). The LiBOB based cell displayed also a lower-voltage discharge plateau and a higher-voltage charge plateau compared to the $LiClO_4$ based batteries (~0.5 V higher overpotential).

All the cells had open circuit voltage (OCV) about 3.2−3.3 V when measuring the cells assembled inside the glovebox. The OCV of the cells increased slightly by 10−40 mV after being filled with oxygen for half an hour. It is expected that OCV drops slowly to the equilibrium OCV (2.9−3.1 V),[33,34] or even to values lower than OCV because of the self-diffusion of Li ions; however, as pointed out in Figure 2, the increase in the OCV continued during the rest time (1 h) before starting the cell-cycling when the cell-container was already filled with oxygen (the inset in Figure 2). The higher OCV of the practical Li−O_2 cells compared to the theoretical equilibrium OCV of the Li−O_2 cell has been referred to as the presence of metal oxide (catalysts) in the carbon cathode.[34] However, a high OCV has also been observed in primary Li−O_2 cells where no catalyst was used.[35,36] The observed increase in OCV during the rest time for Li−O_2 cells using aprotic carbonate electrolytes is unlike the stable OCV of Li−O_2 cells using solid state electrolytes or protected Li anodes.[33,37] Thus, the increase in the OCV of the cells may be explained by side reactions such as oxidation of cathode components (e.g., catalyst, binder etc.) or decomposition of salts or solvents in the presence of oxygen. We have recently shown that $LiPF_6$ salt decompose on the carbon cathode surface already when storing a PC based Li−O_2 cell in the presence of oxygen.[11,31] Diffusion of oxygen gas into the liquid electrolyte, however, may also explain the increase in OCV. Further studies are needed to clarify the origin of high OCV in Li−O_2 cells and its increase during the resting time.

3.2. Surface Characterization of the Carbon Cathode. In the following two sections, we present synchrotron-based PES analysis of the carbon cathode and the Li anode of Li−O_2 cells using 1 M $LiClO_4$ in EC/DEC, 1 M $LiClO_4$ in PC or 1 M LiBOB in PC electrolytes. In all cases, α-MnO_2 nanowire was mixed with the carbon in the porous cathode.

The F 1s and Mn 2p spectra of the cathodes of the cells and also of the pristine cathode are presented in Figure 3. The absence of MnO_2 peaks in the all three Mn 2p spectra of the cycled cathodes shows that a surface layer consisting of reaction products is remaining on the cathode. It should again be noted that the cells were stopped at the charged state. Since the pristine electrode clearly shows the Mn 2p signal, the absence of Mn 2p spectra in the charged cathodes reveals that for all samples a surface layer still remained at the α-MnO_2 surface at the end of charging. The thickness of these surface layers are estimated to be thicker than 1−2 nm.[38] The formation of a surface layer, which remains on α-MnO_2 at the end of charging, would consequently decrease the catalytic activity of α-MnO_2. It has been shown that the role of catalyst in Li−O_2 cells with an aprotic electrolyte is mainly catalyzing the decomposition of electrolytes and formation of CO_2.[7] In other words, observed rechargeability performances in Li−O_2 cells are in fact an effect of electrolyte decomposition during discharging and the α-MnO_2 catalyzes the oxidation of decomposition products during charging. Therefore, covering the α-MnO_2 surface would lead to a decrease of the catalytic activity of α-MnO_2 which could be one explanation to the huge capacity fading in Li−O_2 cells commonly occurring after few cycles. Also, given that there are plenty of electrolyte molecules in the cell and given that the decomposition products formed during the discharge are dominantly removed during charging,[11] the ultimate stop in cycling of the cell is mainly due to the passivation of catalysts by reaction products not lack of electrolyte or blockage of the cathode pores.

dx.doi.org/10.1021/am3026129 | ACS Appl. Mater. Interfaces 2013, 5, 1333−1341

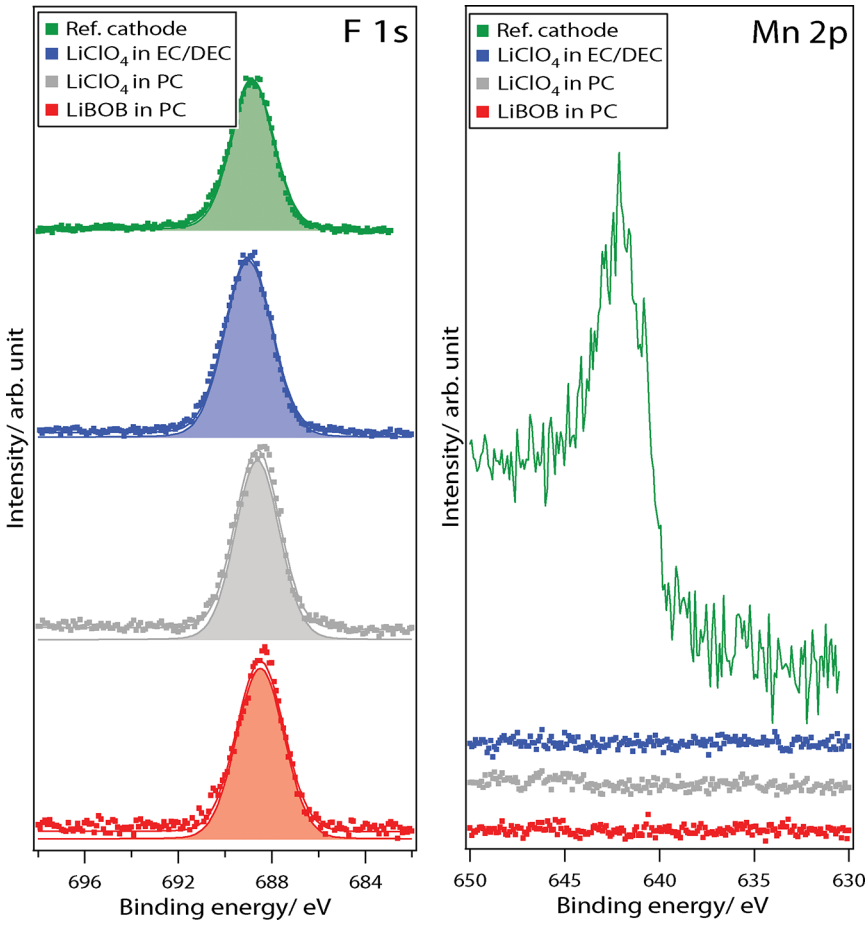

Figure 3. F 1s and Mn 2p spectra of the pristine cathode and the cathode of the Li−O_2 cells at the charged states using electrolytes of 1 M $LiClO_4$ in EC/DEC, 1 M $LiClO_4$ in PC, and 1 M LiBOB in PC.

Previously, we observed a similar formation of surface layers in other Li−O_2 cells at the discharged state using $LiPF_6$ in a PC electrolyte where none of the cathode components (binder, catalyst, and carbon) were visible in the spectra because of formation of a thick surface layer on the cathode surface.[11] Thus, based on the conclusion drawn from the absence of MnO_2 peaks, it may be expected that also the Kynar binder (PVDF-HFP), which is used in the carbon cathode assembly, should be covered by a surface layer and there should be no traces of fluorine in the spectra. However, the F 1s spectra show presence of F in the surface layer of all the three cycled cathodes, similar to the spectrum of the pristine cathode (the binding energy positions of the deconvolved peaks obtained from the cathodes are presented in Table 1 where the peaks are assigned to the compounds using references[9−11,39−41]). The observed F peak is assigned to the binder since this is the only source of F in this system (The C 1s spectra also confirm presence of the binder in the surface layer). Figure 4 shows the SEM micrograph of the pristine carbon cathode and a cycled cathode in a Li−O_2 cell using $LiClO_4$ in PC electrolyte. Here the pristine cathode has a relatively uniform porous structure, while, the cycled cathode hold a rather uniform surface layer between cracks. From these combined results it is proposed that Kynar binder detached (not decomposed) from the porous cathode during battery cycling and that it is involved in the formation of the surface layer present on the cathode surface. The detachment of Kynar may explain the remarkable increase in the brittleness of the carbon cathodes of Li−O_2 cells after

Table 1. Summary of Binding Energy Positions (E_B) and the Assigned Compounds Obtained by the Deconvolution of the XPS Spectra of the Cathodes Presented in Figures 3 and 5 Using Refs 9−11 and 39−41

	E_B (eV)			
peak	$LiClO_4$ in EC/DEC	$LiClO_4$ in PC	LiBOB in PC	assignments
C 1s	285	285	285	$\underline{C}H_3$ (hydrocarbons)
	286.7	286.4	286.3	$\underline{C}H_2CF_2$ (PVDF)
				$\underline{C}$−O (ether bond) in $ROCO_2Li$ and PEO
			289.2	$\underline{C}O_2\underline{C}O_2$ in LiBOB
	289.7	289.6	290.4	$\underline{C}F$ in HFP
				$RO\underline{C}O_2Li$ and/or $Li\underline{C}O_3$
	291.2	291	291	$\underline{C}F_2$ in HFP
				$\underline{C}F_2$ in PVDF
	293.7	293.9	293.6	$\underline{C}F_3$ in HFP
O 1s		530.2		
	532.2	532	532.2	C=$\underline{O}$ in carboxylates and/or carbonates/$LiClO_4$
	533.4	533.3	533.2	C-$\underline{O}$ (ethers)
			534.5	
F 1s	689	688.6	688.5	Kynar
B 1s			192.9	LiBOB
			202.8	
Cl 2p		198.5		$Li\underline{Cl}$
	208.6	208.4		$Li\underline{Cl}O_4$

dx.doi.org/10.1021/am3026129 | ACS Appl. Mater. Interfaces 2013, 5, 1333−1341

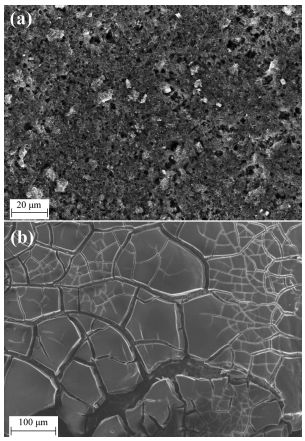

Figure 4. SEM micrograph of pristine (a) and cycled (b) carbon cathode of a Li−O_2 cell using 1 M $LiClO_4$ in PC electrolyte.

cycling. We have observed that the carbon cathodes become very brittle after cell cycling, and therefore, the cathode components can only be kept together by using a mesh as a substrate of the cathode components, unlike the pristine carbon cathodes that could be made as a paper and handled easily without the mesh. The Kynar binder degradation in the Li−O_2 battery has recently been discussed in the literature.[13,17,42] However, the presented results in this study do not suggest defluorination of Kynar in the cells since no LiF peak (at 685 eV) is present in the F 1s spectra. The results rather suggest detachment and deformation of the Kynar in these PC and EC/DEC based cells. It has also been shown that detached Kynar binder is transported from the cathode side to the anode side and found to be present in the SEI of the Li anode.[31]

The C 1s spectra (Figure 5) of the cathodes of $LiClO_4$-based cells ($LiClO_4$ in EC/DEC or PC) consist of 5 peaks at binding energies of 285, 286.7, 289.7, 291.2, and 293.7 eV, respectively, indicating presence of at least five different carbon bonding environments. The peak at the highest binding energy, at 293.7 eV in the C 1s spectra, originates from the HFP part of the Kynar binder. The contribution of this peak is equal to 9.7 and 2.6% of the total area of the C 1s spectra for the EC/DEC and PC samples, respectively (Figure 5). The same relative contribution from HFP is expected for the CF_2 peak at 291.2 eV, because the atomic percentage of CF_3 and CF_2 is the same in the HFP. Therefore, by subtracting the contribution of HFP in the CF_2 peak, we can estimate the relative contribution of PVDF to the CF_2 peak (17.2 and 15.6% of the total area of the C 1s spectra of the EC/DEC and PC samples, respectively). Similarly, the relative contribution of ether bonds (−C−O−) and CH_2 of PVDF to the peak at 286.7 eV is estimated to 10.6% (27.8−17.2%) and 25.8% (41.4−15.6%) for the $LiClO_4$ in EC/DEC and $LiClO_4$ in PC samples, respectively. The relative contribution of each chemical compound to the C 1s spectra is presented in Figure 6. Compared to the $LiClO_4$ in the PC cell, the $LiClO_4$ in EC/DEC displays relatively higher amounts of binder and lower amounts of carbonates and ethers on the surface of the carbon cathode. This indicates that the decomposition products of $LiClO_4$ in PC electrolyte are present on the surface layer to a larger extent compared to the decomposition products of $LiClO_4$ in the EC/DEC electrolyte.

The C 1s peak at 289.7 eV shows the presence of carbonate species remaining on the surface layer of the $LiClO_4$-based cells after charging. It has been demonstrated that Li_2CO_3 and $ROCO_2Li$ (lithium alkyl carbonate) are among the suggested discharge products of the carbonate-based compounds.[11,16] It has particularly been shown that $CH_3CH_2OCO_2Li$ (lithium

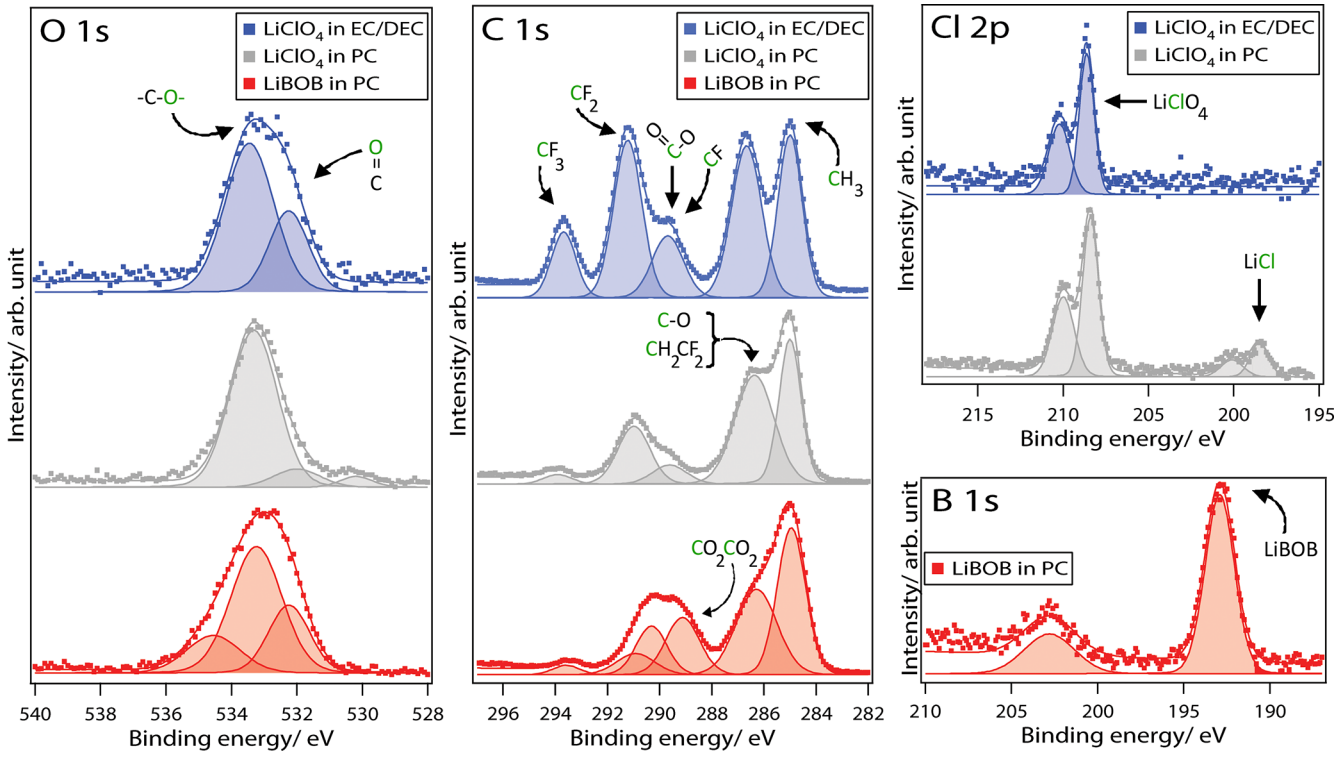

Figure 5. O1s, C 1s, Cl 2p, and B 1s spectra of the cathode of the Li−O_2 cells at charged states using 1 M $LiClO_4$ in EC/DEC, 1 M $LiClO_4$ in PC, or 1 M LiBOB in PC electrolytes.

dx.doi.org/10.1021/am3026129 | ACS Appl. Mater. Interfaces 2013, 5, 1333−1341

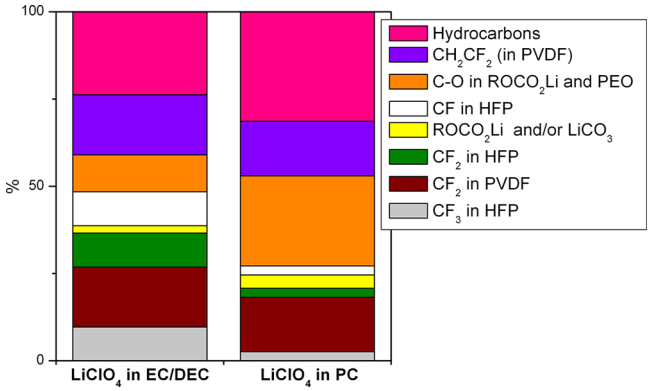

Figure 6. Relative molecular percentage of C-containing compounds on the surface of the cathodes at the charged states using $LiClO_4$ in EC/DEC or in PC electrolytes.

ethyl carbonate) form due to the decomposition of EC/DEC electrolyte in the Li−O_2 battery.[43] The carbonate bond (−CO_3) in any of these compounds is contributing to the carbonate peak at 289.7 eV.

Assuming formation of these compounds, the C 1s spectra of both EC/DEC based samples show that the relative amounts of ether compounds are higher compared to the relative amounts of carbonate compounds. The O 1s spectra also confirm the higher relative amount of the ether peak compared to the carbontes/carboxylates. The peak at 533.3 eV representing ethers has also a bigger contribution to the O 1s spectra compared to the peak at 532 eV representing carbonates and carboxylates. The higher relative amount of ethers to carbonates could be attributed to the formation of polyethylene oxide (PEO) $(-CH_2-CH_2-O-)_n$ on the surface layer.[9] The presence of this compound in the surface of the Li anode of a Li−O_2 battery using $LiPF_6$ in PC electrolyte has also previously been reported.[31]

The Cl 2p spectra are deconvoluted using spin−orbit split doublets for each chemical state (Cl $2p_{3/2}$ and Cl $2p_{1/2}$) with an intensity ratio 2:1 and a peak split of 1.6 eV.[44] The Cl 2p spectrum of the EC/DEC sample contains one peak assigned to the $LiClO_4$ salt in the surface layer. However, the Cl 2p spectrum of the PC sample shows two peaks assigned to LiCl and $LiClO_4$. The LiCl peak indicates the decomposition of $LiClO_4$. Therefore, the Cl 2p spectra reveal that the decomposed $LiClO_4$ is present in the surface layer of cathode of a Li−O_2 battery when using a PC solvent while not when using an EC/DEC solvent. $LiClO_4$ has been suggested to be a more stable salt compared to $LiPF_6$ or $LiBF_4$ in the Li−O_2 battery.[12,18]

The C 1s spectrum of the cathode of the LiBOB in PC cell is somewhat different from that of the $LiClO_4$ based cells. One additional peak at 289.2 eV representing carboxylates on the surface of the carbon cathode appeared in the C 1s spectrum. This peak originates from the CO_2CO_2 bond of the LiBOB and indicates the presence of residual amounts of LiBOB although the samples were washed prior to the XPS measurements. The B 1s spectrum of this sample, which consists of two peaks, supports this finding. The peak at lower binding energy, at 192.9 eV, in the B 1s spectrum indicates the presence of LiBOB. However, the B 1s peak at higher binding energy (202.8 eV) suggests decomposition of LiBOB. This peak, with relatively high binding energy, indicates that B atoms are bound to highly electronegative substitution like $-CF_3$. However, at this stage, we cannot assign any specific compound to this peak.

The results clearly demonstrate the appearance of decomposition products of both $LiClO_4$ and LiBOB salts on the carbon cathode surface in the PC based cells, whereas $LiClO_4$ showed to be stable in the EC/DEC-based cell.

3.3. Surface Characterization of the Li Anode. The SEI of the Li anode protects electrolyte from further decomposition, however, it has been shown that the presence of oxygen influences the SEI.[31] With $LiPF_6$ in PC electrolyte, the presence of oxygen results in the formation of an unstable SEI that evolves during the cycling. Furthermore, the presence of oxygen increases the resistance of the cell.[31]

Here, we investigate the surface of the Li anode of Li−O_2 cells with $LiClO_4$ based electrolytes. Figure 7 shows photographs of the pristine Li foil and the Li anode after cycling using $LiClO_4$ in PC. It can be seen that the surface of the Li anode changed significantly from a shiny smooth surface to a rough black surface layer. This is similar to the previously reported photograph of the Li anode from a Li−O_2 cell.[45]

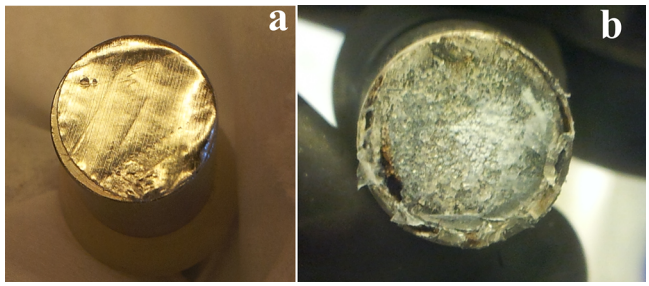

Figure 7. Photograph of (a) pristine and (b) cycled Li anode in a Li−O_2 cell.

The PES spectra of the Li anodes of the cycled Li−O_2 cells using $LiClO_4$ in EC/DEC or PC electrolyte are presented in Figure 8. The F 1s spectra show one main contribution albeit a nonfluorinated salt, $LiClO_4$, was used to cycle the cells. The binding energy of this peak matches to the binding energy of Kynar and thus suggests that Kynar was transported from the cathode to the Li anode. This supports the conclusion presented above indicating detachment of Kynar binder from the carbon cathode. It should be mentioned that we are aware of the possibility of the presence of F contamination on Li anode. However, our previous results showed that this peak assigned to Kynar appeared on the Li anode solely in the charged state and not in the discharged or stored states of the cells, where the spectra are expected to be more influenced by F contaminations.[31] Therefore, the observed F 1s peak in the anode of the $LiClO_4$ batteries most likely originates from the transported Kynar binder.

It should be noted that the small peak at 685 eV was also observed in the F 1s spectrum of the Li anode of the PC sample (Figure 8), indicating the presence of some LiF. However, the relative intensity of this peak was increasing during the PES measurement suggesting that the peak may have been formed because of radiation damage.

The C 1s spectra of both anodes display four peaks representing hydrocarbon, ethers, carboxylates and carbonates from the lowest to the highest binding energies (Table 2). The carbonate peak originates from either; i) solvents remaining on the surface, and/or ii) from solvent molecules that have been decomposed forming Li_2CO_3 and/or $ROCO_2Li$ species. As

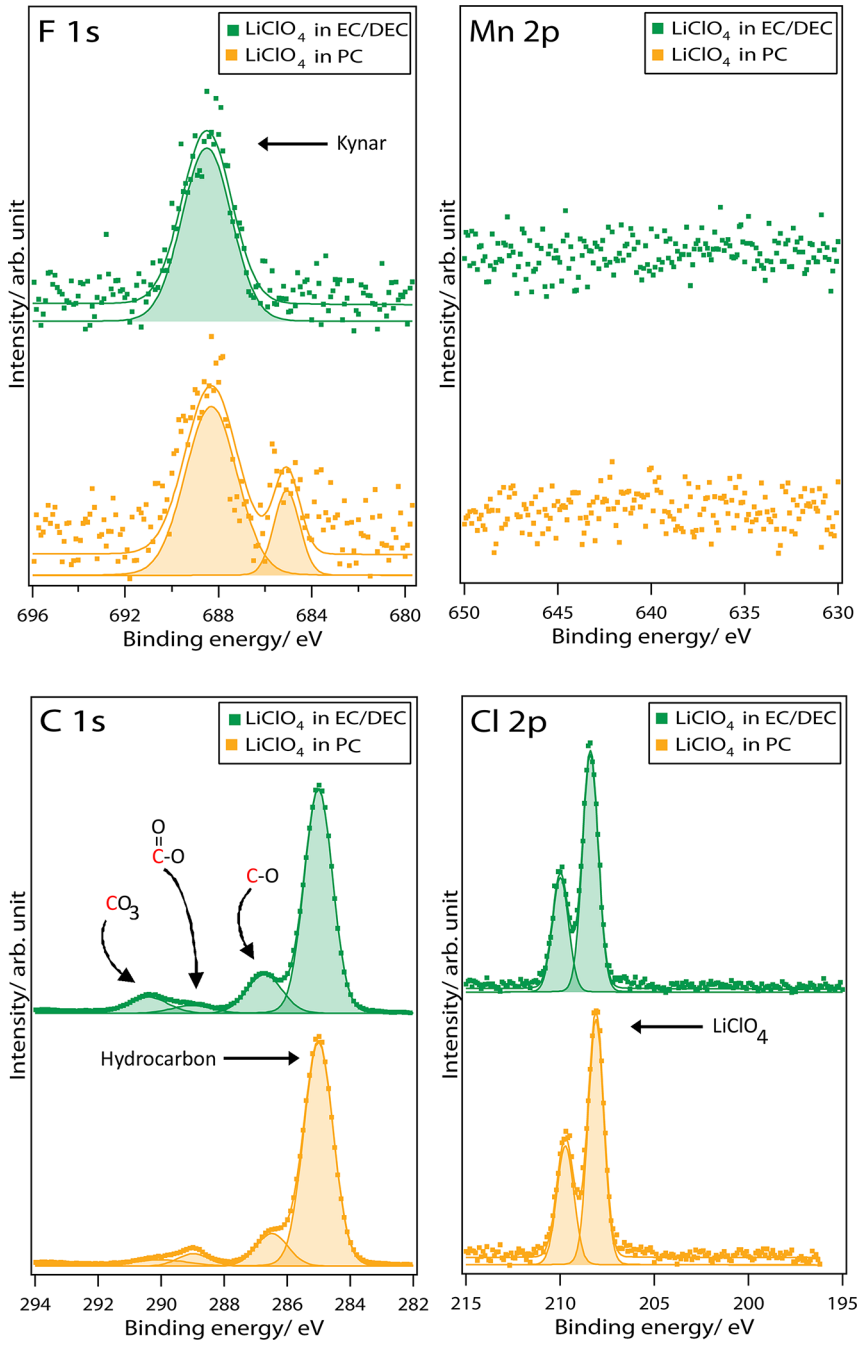

Figure 8. F 1s, Mn 2p, C 1s, and Cl 2p spectra of the Li anodes in Li−O_2 cells at the charged state using 1 M $LiClO_4$ in EC/DEC or PC electrolytes, respectively.

calculated from the C 1s spectra, the relative amount of ether is higher than the relative amount of carbonates on the surfaces of both anodes. The ratio of the relative amounts of ether:-carbonate is almost equal to 2:1 for the Li anode of the EC/DEC cell. This ratio is the same as the ratio of ether:carbonate in the molecular structure of the EC/DEC solvent. However, the ratio is higher (almost 3:1) for the Li anode cycled in PC indicating that more PEO compounds were present in the SEI of the Li anode cycled in PC. The relative amount of carboxylates, which originates from the decomposition of electrolyte, is larger on the Li anode cycled with PC than that cycled with EC/DEC.

Considering all these results, the spectra therefore suggest that compared to EC/DEC, PC decomposes to a larger degree to PEO compounds. The C 1s spectra also show that the SEI chemistry on the Li anode depends on the solvent chemistry.

The Cl 2p spectra display one peak at 208.4 eV revealing the presence of $LiClO_4$ salt in the SEI. Interestingly, no LiCl, which indicates decomposition of $LiClO_4$, was observed on the surface of the Li anodes.

Taken together, the results indicate that the decomposed solvents in addition to $LiClO_4$ salt contribute to the formation of the SEI on the Li anode in the presence of oxygen. However, no decomposition product of $LiClO_4$ influenced the SEI on the Li anodes.

dx.doi.org/10.1021/am3026129 | ACS Appl. Mater. Interfaces 2013, 5, 1333−1341

Table 2. Summary of the Binding Energy Positions (E_B) Obtained in the Deconvolution of the Spectra of the Li Anodes Presented in Figures 8 and the Assigned Compounds

	E_B (eV)		
peak	1 M $LiClO_4$ in EC/DEC	1 M $LiClO_4$ in PC	assignments
C 1s	285	285	hydrocarbon (C−H)
	286.7	286.5	C−O (ethers)/CH_2 of Kynar
	289	289	O−C═O (carboxylates)
	290.4	290	CO_3 (carbonates)
F 1s	688.5	688.3	Kynar
Cl 2p	208.4	208.1	$LiClO_4$

4. CONCLUSIONS

The PES study revealed that a surface layer remains on the surfaces of both carbon cathode and Li anode of cycled Li−O_2 cells at the charged (delithiated) state using $LiClO_4$ or LiBOB in PC or EC/DEC electrolytes. Both PC and EC:DEC (1:1) solvents decompose during the cycling and form carbonate and ether containing species on the carbon cathode. However, less decomposition products were detected on the carbon cathode surface when cycled with EC/DEC than on that cycled with PC. The results also showed that both the $LiClO_4$ and LiBOB salts decompose when cycled in a PC based Li−O_2 cell and contribute to formation of surface layers on the cathode surface. However, we did not observe any $LiClO_4$ salt decomposition when cycling in the EC:DEC (1:1) electrolyte. The absence of α-MnO_2 peaks and the presence of a Kynar binder peak in the PES spectra of the carbon cathodes imply that; (i) a surface layer forms and remains on the surface of the α-MnO_2 catalyst; and/or (ii) Kynar binder detaches from the cathode and covers the MnO_2 catalyst during the cell cycling. In both cases the catalytic activity of MnO_2 decreases due to the formation of the surface layer. The thickness of the surface layer is estimated to be at least 1−2 nm thick. The surface characterizations indicate that at the charged state of a Li−O_2 cell with $LiClO_4$ in PC or EC/DEC electrolytes, the SEI of Li anode is made of PEO, carboxylates, carbonates, and $LiClO_4$ salt. No decomposition products from the $LiClO_4$ salt were observed in the SEI of Li anodes.

AUTHOR INFORMATION

Corresponding Author

*E-mail: reza.younesi@kemi.uu.se. Tel: +46 18 471 3769.

Notes

The authors declare no competing financial interest.

ACKNOWLEDGMENTS

The authors acknowledge financial support from the Swedish Energy Agency (STEM), the Swedish Research Council (VR), and StandUp for Energy. Rebecka Lindblad, Uppsala University, is gratefully acknowledged for her support with measuring a reference sample at the MaxLab IV Laboratory, Lund.

REFERENCES

(1) Abraham, K. M. *J. Electrochem. Soc.* **1996**, *143*, 1−5.
(2) Hou, J.; Yang, M.; Ellis, M. W.; Moore, R. B.; Yi, B. *Phys. Chem. Chem. Phys.* **2012**, *14*, 13487−13501.
(3) Hardwick, L. J.; Bruce, P. G. *Curr. Opin. Solid State Mater. Sci.* **2012**, *16*, 178−185.
(4) Shao, Y.; Park, S.; Xiao, J.; Zhang, J.-G.; Wang, Y.; Liu, J. *ACS Catal.* **2012**, *2*, 844−857.
(5) Cao, R.; Lee, J.-S.; Liu, M.; Cho, J. *Adv. Energy Mater.* **2012**, *2*, 816−829.
(6) Kichambare, P.; Rodrigues, S.; Kumar, J. *ACS Appl. Mater. Interfaces* **2012**, *4*, 49−52.
(7) McCloskey, B. D.; Scheffler, R.; Speidel, A.; Bethune, D. S.; Shelby, R. M.; Luntz, A. C. *J. Am. Chem. Soc.* **2011**, *133*, 18038−18041.
(8) Lu, Y.-C.; Gasteiger, H. a.; Parent, M. C.; Chiloyan, V.; Shao-Horn, Y. *Electrochem. Solid-State Lett.* **2010**, *13*, A69−A72.
(9) Andersson, A. M.; Edström, K. *J. Electrochem. Soc.* **2001**, *148*, A1100−A1109.
(10) Andersson, A. M.; Herstedt, M.; Bishop, A. G.; Edström, K. *Electrochim. Acta* **2002**, *47*, 1885−1898.
(11) Younesi, R.; Urbonaite, S.; Edström, K.; Hahlin, M. *J. Phys. Chem. C* **2012**, *116*, 20673−20680.
(12) Veith, G. M.; Nanda, J.; Delmau, L. H.; Dudney, N. J. *J. Phys. Chem. Lett.* **2012**, *3*, 1242−1247.
(13) Younesi, R.; Hahlin, M.; Treskow, M.; Scheers, J.; Johansson, P.; Edström, K. *J. Phys. Chem. C* **2012**, *116*, 18597−18604.
(14) Hyoung, Oh, S.; Yim, T.; Pomerantseva, E.; Nazar, L. F. *Electrochem. Solid-State Lett.* **2011**, *14*, A185−A188.
(15) Laoire, C. O.; Mukerjee, S.; Abraham, K. M.; Plichta, E. J.; Hendrickson, M. A. *J. Phys. Chem. C* **2010**, *114*, 9178−9186.
(16) Freunberger, S. A.; Chen, Y.; Peng, Z.; Griffin, J. M.; Hardwick, L. J.; Bardé, F.; Novák, P.; Bruce, P. G. *J. Am. Chem. Soc.* **2011**, *133*, 8040−8047.
(17) Younesi, R.; Hahlin, M.; Björefors, F.; Johansson, P.; Edström, K. *Chem. Mater.* **2013**, *25*, 77−84.
(18) Oswald, S.; Mikhailova, D.; Scheiba, F.; Reichel, P.; Fiedler, A.; Ehrenberg, H. *Anal. Bioanal. Chem.* **2011**, *400*, 691−696.
(19) McCloskey, B. D.; Bethune, D. S.; Shelby, R. M.; Mori, T.; Scheffler, R.; Speidel, A.; Sherwood, M.; Luntz, A. C. *J. Phys. Chem. Lett.* **2012**, *3*, 3043−3047.
(20) Chalasani, D.; Lucht, B. L. *ECS Electrochem. Lett.* **2012**, *1*, A38−A42.
(21) Hassoun, J.; Croce, F.; Armand, M.; Scrosati, B. *Angew. Chem., Int. Ed.* **2011**, *50*, 2999−3002.
(22) De Giorgio, F.; Soavi, F.; Mastragostino, M. *Electrochem. Commun.* **2011**, *13*, 1090−1093.
(23) Peng, Z.; Freunberger, S. A.; Chen, Y.; Bruce, P. G. *Science* **2012**, *337*, 563−566.
(24) Mizuno, F.; Nakanishi, S.; Shirasawa, A.; Takechi, K.; Shiga, T.; Nishikoori, H.; Iba, H. *Electrochemistry* **2011**, *79*, 876−881.
(25) Wang, H.; Xie, K.; Wang, L.; Han, Y. *J. Power Sources* **2012**, *219*, 263−271.
(26) Zhang, Z.; Lu, J.; Assary, R. S.; Du, P.; Wang, H.-H.; Sun, Y.-K.; Qin, Y.; Lau, K. C.; Greeley, J.; Redfern, P. C.; Iddir, H.; Curtiss, L. A.; Amine, K. *J. Phys. Chem. C* **2011**, *115*, 25535−25542.
(27) Mizuno, F.; Nakanishi, S.; Kotani, Y.; Yokoishi, S.; Iba, H. *Electrochemistry* **2010**, *78*, 403−405.
(28) Xu, W.; Hu, J.; Engelhard, M. H.; Towne, S. A.; Hardy, J. S.; Xiao, J.; Feng, J.; Hu, M. Y.; Zhang, J.; Ding, F.; Gross, M. E.; Zhang, J.-G. *J. Power Sources* **2012**, *215*, 240−247.
(29) Veith, G. M.; Dudney, N. J.; Howe, J.; Nanda, J. *J. Phys. Chem. C* **2011**, *115*, 14325−14333.
(30) Takechi, K.; Higashi, S.; Mizuno, F.; Nishikoori, H.; Iba, H.; Shiga, T. *ECS Electrochem. Lett.* **2012**, *1*, A27−A29.
(31) Younesi, R.; Hahlin, M.; Roberts, M.; Edström, K. *J. Power Sources* **2013**, *225*, 40−45.
(32) Luo, J.; Zhu, H. T.; Fan, H. M.; Liang, J. K.; Shi, H. L.; Rao, G. H.; Li, J. B.; Du, Z. M.; Shen, Z. X. *J. Phys. Chem. C* **2008**, *112*, 12594−12598.
(33) Kumar, B.; Kumar, J.; Leese, R.; Fellner, J. P.; Rodrigues, S. J.; Abraham, K. M. *J. Electrochem. Soc.* **2010**, *157*, A50.
(34) Zhang, S. S.; Ren, X.; Read, J. *Electrochim. Acta* **2011**, *56*, 4544−4548.

(35) Younesi, S. R.; Urbonaite, S.; Björefors, F.; Edström, K. *J. Power Sources* **2011**, *196*, 9835−9838.
(36) Zhang, S. S.; Foster, D.; Read, J. *J. Power Sources* **2010**, *195*, 1235−1240.
(37) Zhang, T.; Imanishi, N.; Hasegawa, S.; Hirano, A.; Xie, J.; Takeda, Y.; Yamamoto, O.; Sammes, N. *Electrochem. Solid-State Lett.* **2009**, *12*, A132−A135.
(38) Seah, M. P. *Surf. Interface Anal.* **2012**, *44*, 497−503.
(39) Herstedt, M.; Andersson, A. M.; Rensmo, H.; Siegbahn, H.; Edström, K. *Electrochim. Acta* **2004**, *49*, 4939−4947.
(40) Nazri, G.; Muller, R. M. *J. Electrochem. Soc.* **1985**, *132*, 2050−2054.
(41) Verma, P.; Maire, P.; Novák, P. *Electrochim. Acta* **2010**, *55*, 6332−6341.
(42) Black, R.; Oh, S. H.; Lee, J.-H.; Yim, T.; Adams, B.; Nazar, L. F. *J. Am. Chem. Soc.* **2012**, *134*, 2902−2905.
(43) Wang, H.; Xie, K. *Electrochim. Acta* **2012**, *64*, 29−34.
(44) Moulder, J. F., Stickle, W. F., Sobol, P. E., Bomben, K. D. *Handbook of X-ray Photoelectron Spectroscopy*; Chastain, J., King, R. C., Eds.; Physical Electronics: Eden Prairie, MN, 1992.
(45) Laoire, C. O.; Mukerjee, S.; Plichta, E. J.; Hendrickson, M. A.; Abraham, K. M. *J. Electrochem. Soc.* **2011**, *158*, A302−A308.